Supplement of

Evolution of firework-related barium aerosols: insights from single-particle analysis and mass concentration monitoring

Xiufeng Lian[1, 2], Chenglei Pei[3], Wei Sun[4], Chen Lv[5], Kunlun Huang[3], Lei Lei[3], Bo Huang[2], Chunlei Cheng[1], Guohua Zhang[4], Xinhui Bi[4], Zhen Zhou[1], Mei Li[1,*]

1 College of Environment and Climate, Institute of Mass Spectrometry and Atmospheric Environment, Guangdong Provincial Engineering Research Center for On-line Source Apportionment System of Air Pollution, Jinan University, Guangzhou 510632, China

2 Guangzhou Hexin Instrument Co., Ltd., Guangzhou 510530, China

3 Guangzhou Sub-branch of Guangdong Ecological and Environmental Monitoring Center， Guangzhou 510006, China

4 State Key Laboratory of Organic Geochemistry and Guangdong Provincial Key Laboratory of Environmental Protection and Resources Utilization, Guangzhou Institute of Geochemistry, Chinese Academy of Sciences, Guangzhou 510640, China

[5] College of Ecology and Environment, Zhengzhou University, Zhengzhou 450001, China

[*]Correspondence to: Mei Li (*limei@jnu.edu.cn*)

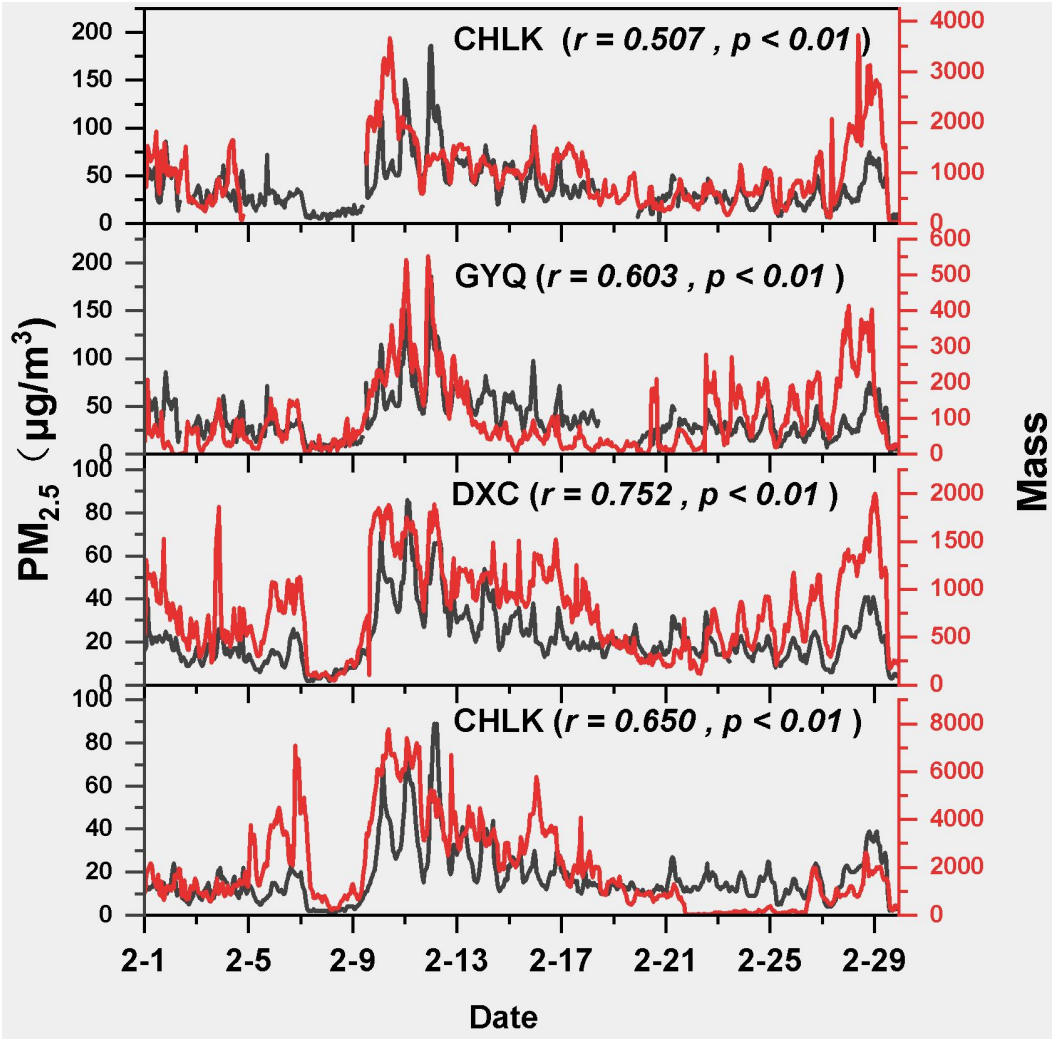

Fig.ure S1. The time series and correlations of the number of Ba-containing single particles and $PM_{2.5}$ mass concentration at the four monitoring stations

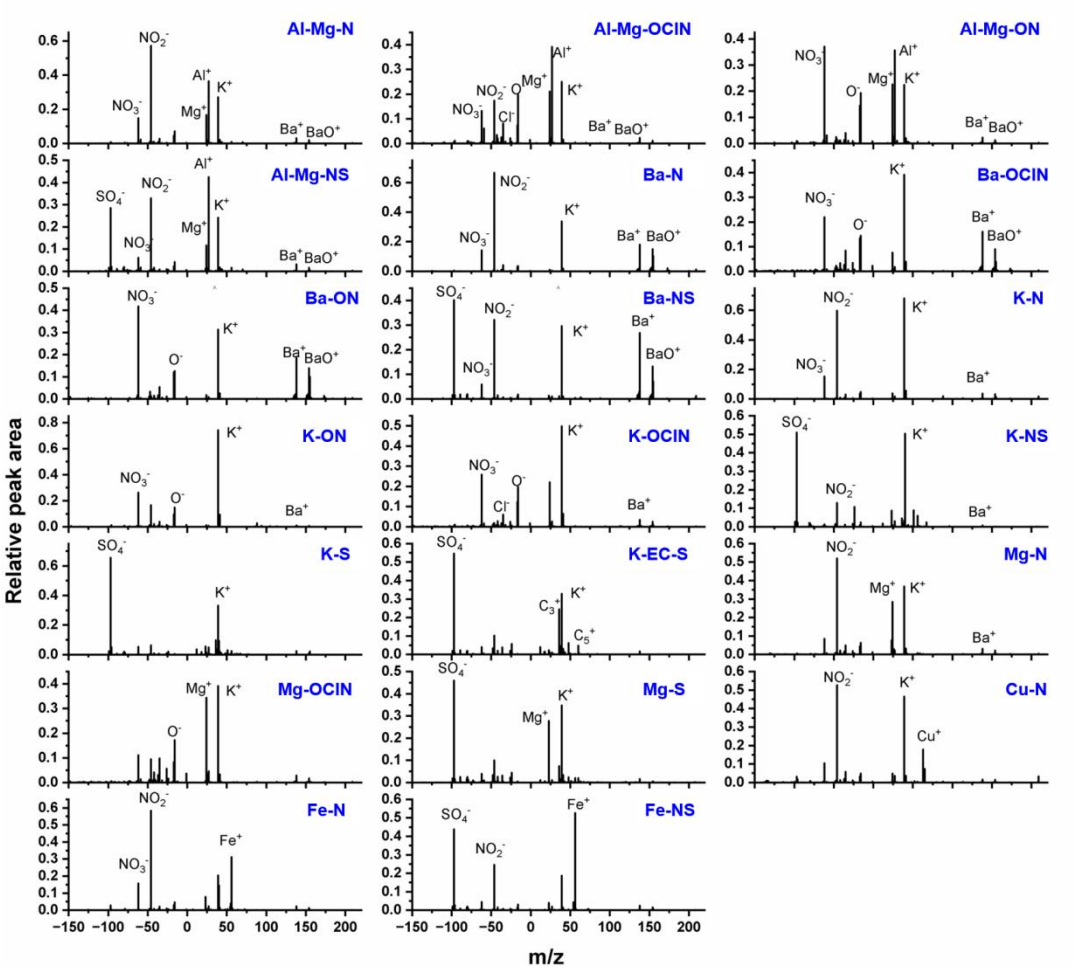

20 **Figure S2. Average mass spectra for the main Ba-containing particle types.**

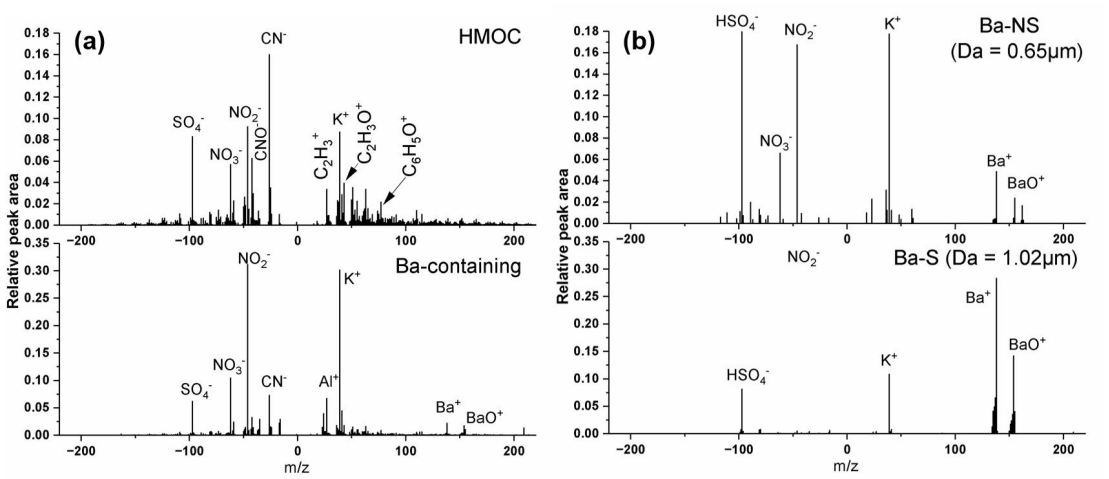

Figure S3. (a)The average mass spectrum of the high-molecular-weight organic (HMOC) type particles and Ba-containing particles; (b) Representative property spectra of Ba-N-S and Ba-S particle types during FI.

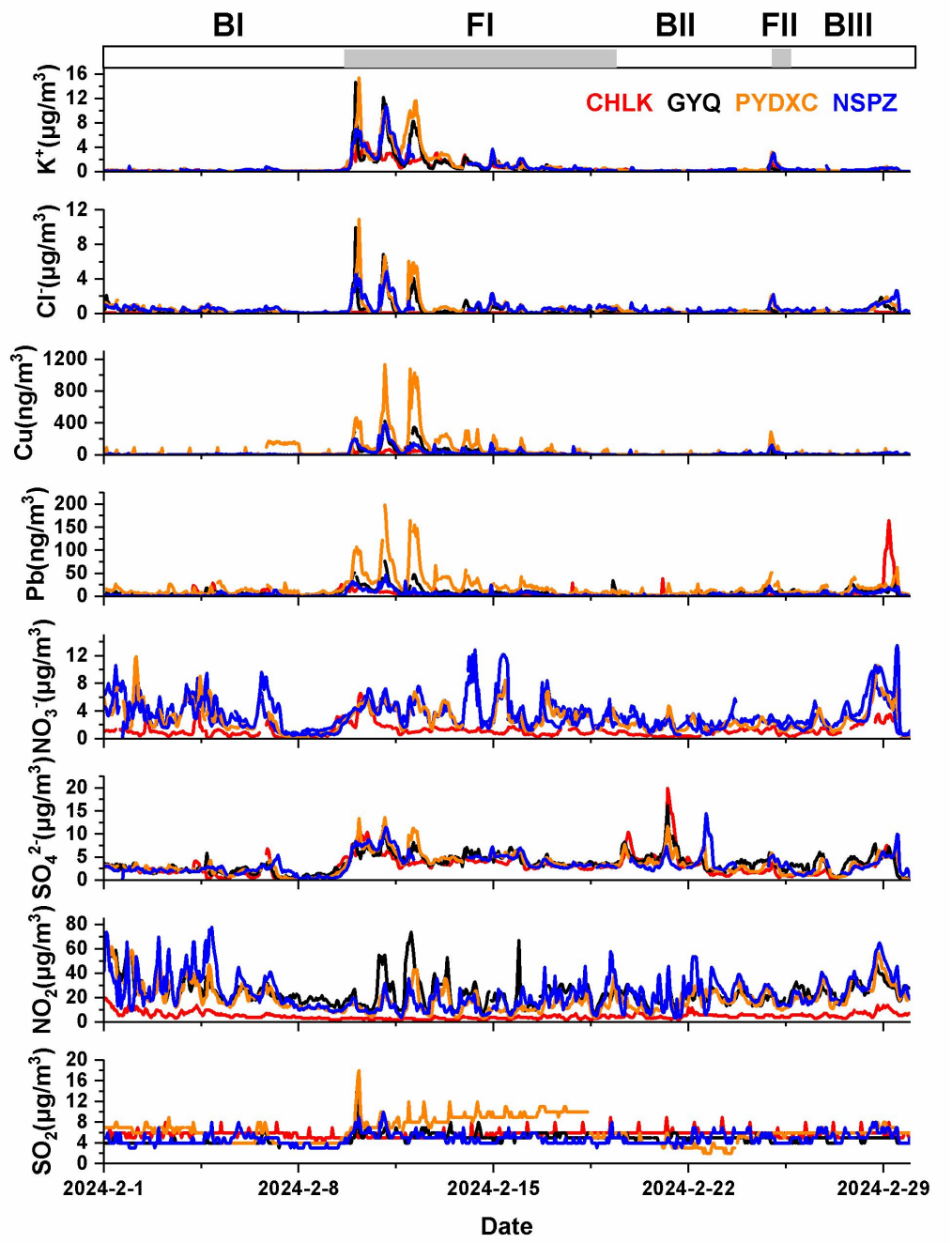

25 **Figure S4. Synchronous time curves of potassium ion (K^+), chloride ion (Cl^-), copper (Cu), lead(Pb), nitrate (NO_3^-), sulfate (SO_4^{2-}), NO_2, and SO_2 concentrations at the four monitoring sites.**

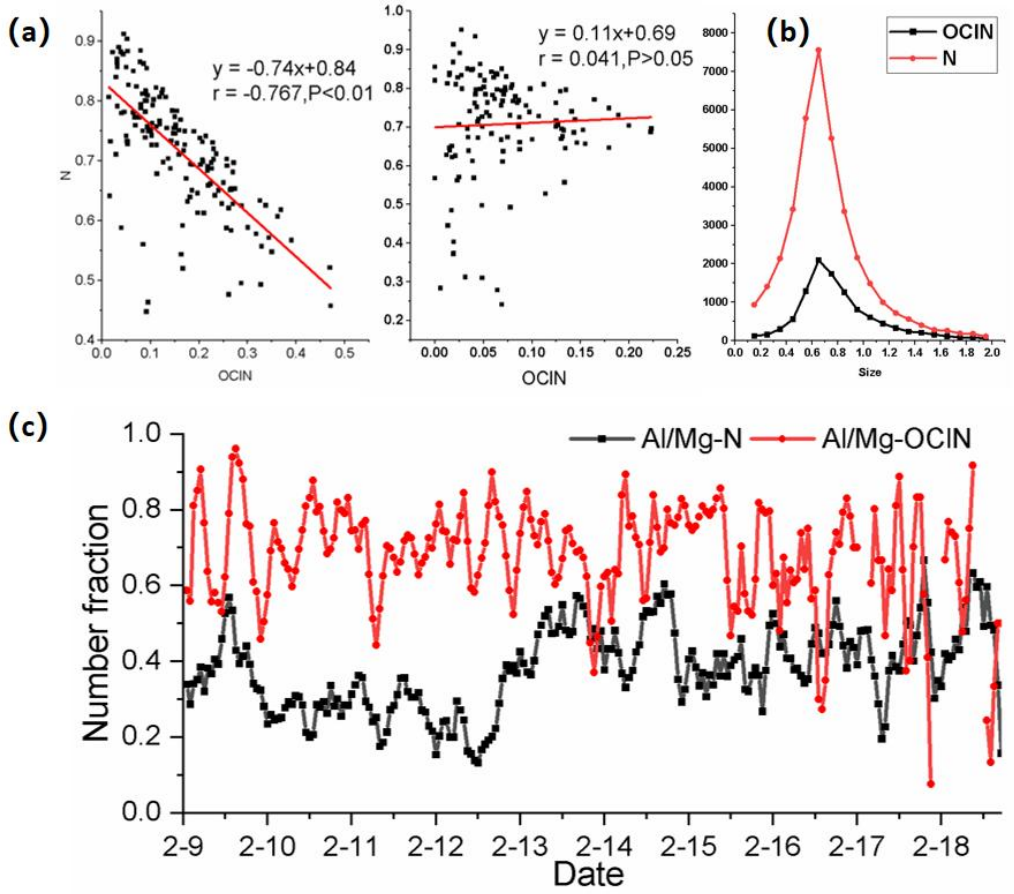

Figure S5. (a) The correlation between the average quantities of N-type particles and OClN-type particles at the four stations during the period from February 9th to 15th (left graph) and from February 16th to 19th (right graph); (b) Particle size distribution diagrams of N type particles and OClN type particles; (c) The time series graph showing the proportion of Al or Mg mixed particles in N-type and OClN-type particles respectively during the FI period.

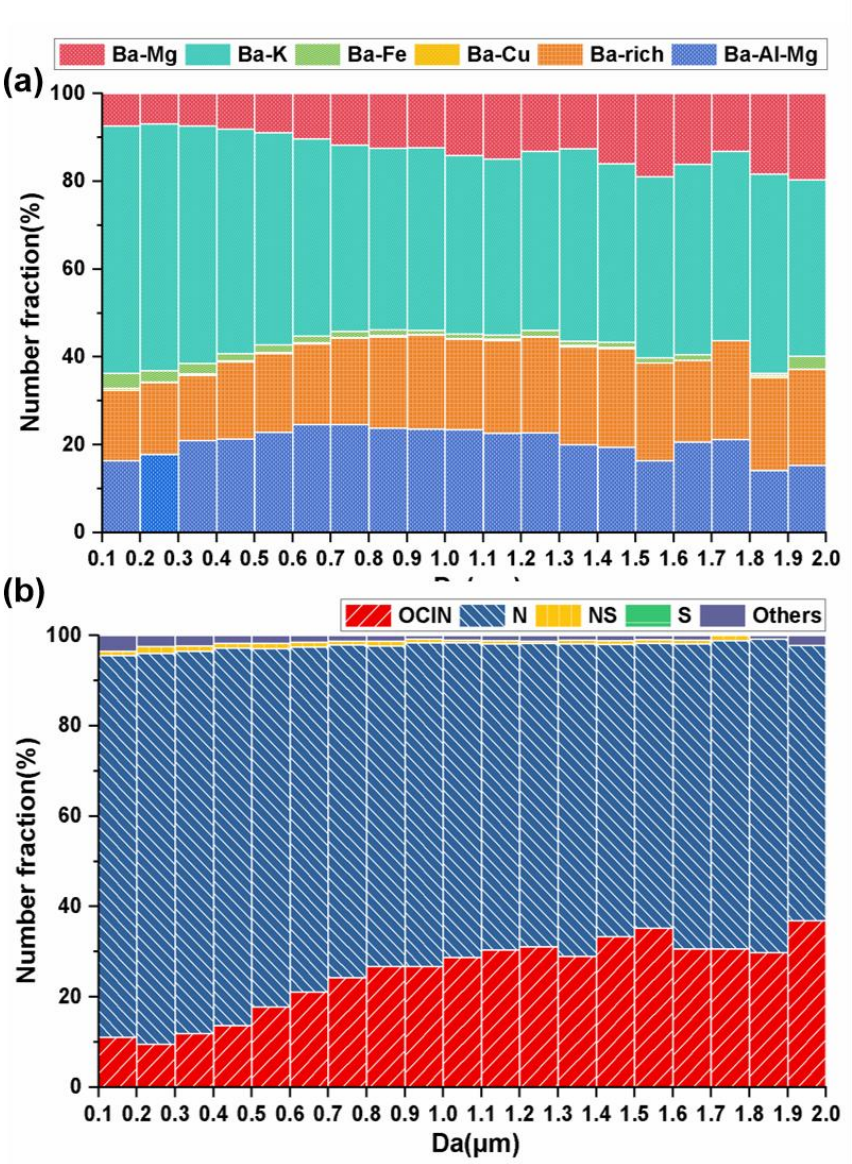

Figure S6. The relative number fractions and size distribution of the main types of Ba-containing particles. (a) Classification based on positive ion mass spectra; (b) Classification based on negative ion mass spectra.

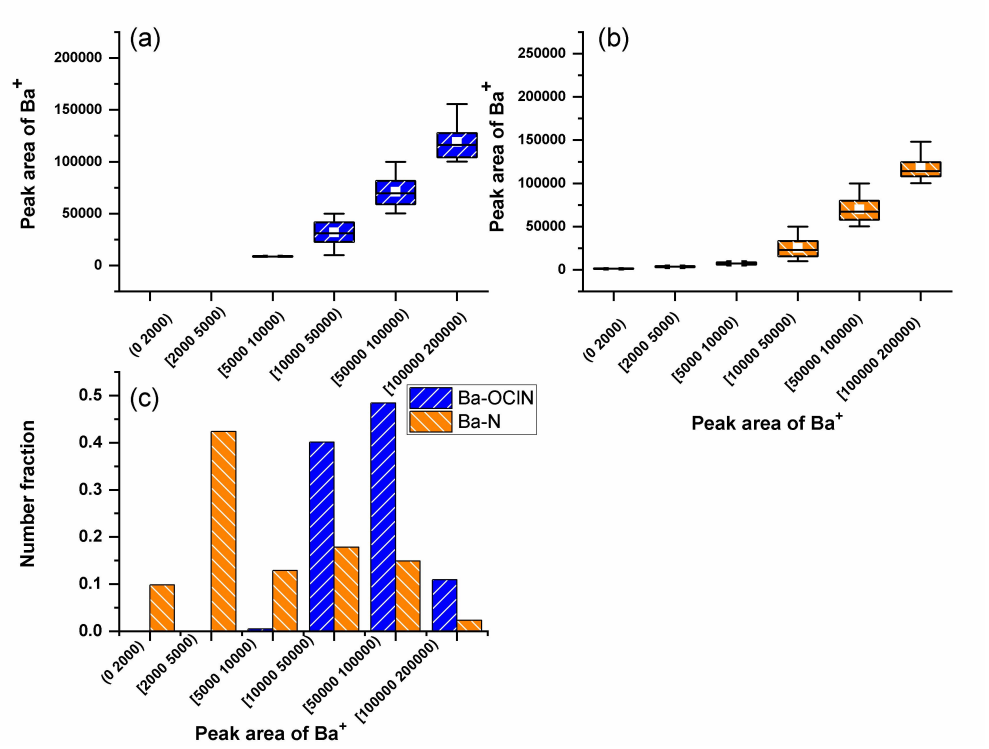

35

Figure S7. (a, b) Box plots of single-particle Ba peak areas by interval for Ba-OClN and Ba-N particles at the Nansha Puzhou site; (c) Number fraction of particles in each interval at the same site.

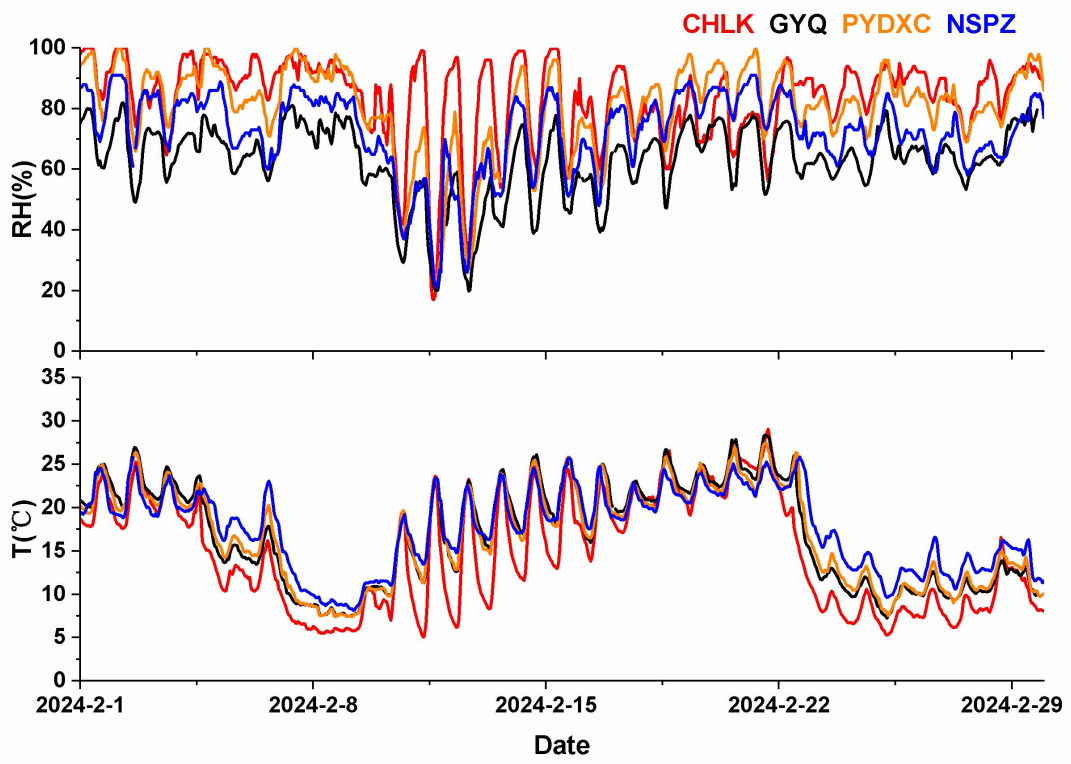

Figure S8. The time series of relative humidity (RH) and temperature(T) at the four sampling sites during the sampling period.